Electronic Supplementary Material (ESI) for Journal of Materials Chemistry A.

Supporting Information

Optimization of tannin-derived hard carbon spheres for high performance sodium-ion batteries

Adrian Beda,[a,b,c] François Rabuel,[c,d] Omar Rahmouni,[a,b] Mathieu Morcrette[c,d] and Camélia Matei Ghimbeu [a,b,c,*]

[a] Université de Haute-Alsace. CNRS. Institut de Science des Matériaux de Mulhouse (IS2M) UMR 7361. F-68100 Mulhouse. France

[b] Université de Strasbourg. F-67081 Strasbourg. France

[c] Réseau sur le Stockage Electrochimique de l'Energie (RS2E). HUB de l'Energie. FR CNRS 3459. 80039 Amiens Cedex. France

[d] Université de Picardie Jules Verne. Laboratoire de Réactivité et Chimie des Solides (LRCS). UMR 7314 CNRS. HUB de l'Energie. 80039 Amiens. France

* E-mail: camelia.ghimbeu@uha.fr

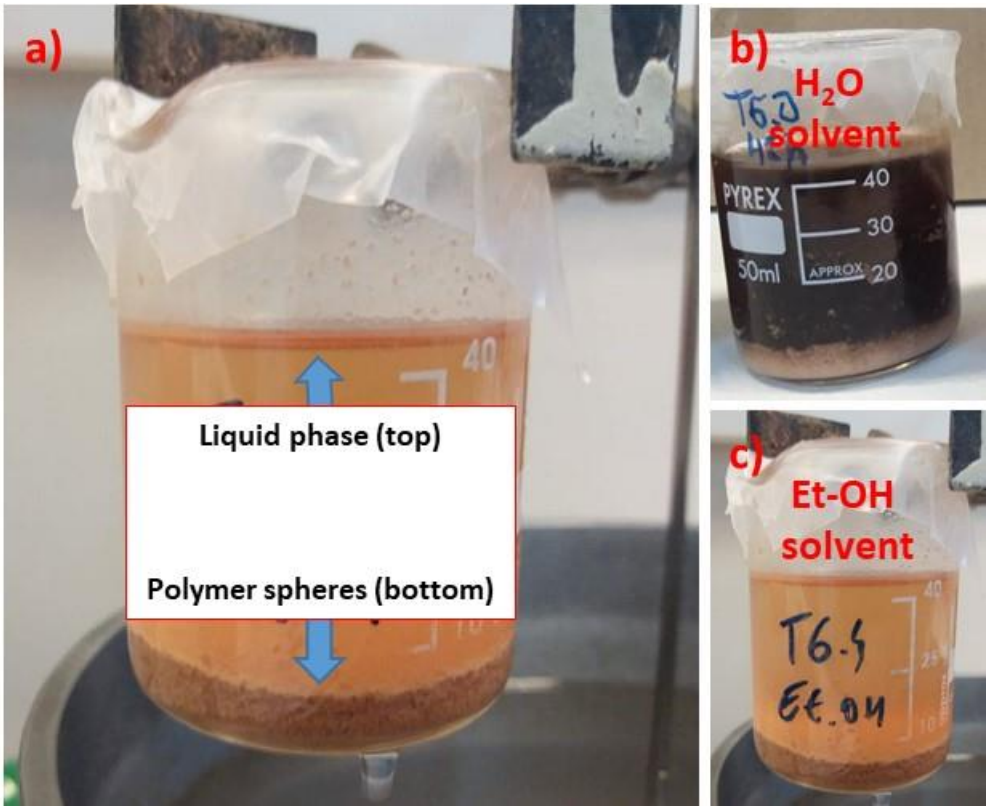

Figure S1: Polymer solutions after 48h reaction time: a) liquid phase on top to be discarded and the polymer spheres formed on the bottom side; b) solution obtained with H_2O solvent and c) solution obtained with Et-OH solvent.

Table S1. Synthesis conditions used for optimization of polyphenol spheres. Only one parameter was varied at a time, and the name of the sample was given according to the parameter studied.

Studied parameter	Polymer name	Solvent type	C-L* 1 type	C-L* 2 mass	C-L* 2 type	Synthesis time (h)
-	Reference[#]	H_2O	GA	0.5	TEDA	48
Solvent	Et-OH	Et-OH	GA	0.5	TEDA	48
	H_2O/Et-OH	H_2O/Et-OH	GA	0.5	TEDA	48
Cross-linker	GL/TEDA	H_2O	GL	0.5	TEDA	48
	GA/TEDA	H_2O	GA	0.5	HMTA	48
Amount of C-L* 2	0.3 g TEDA	H_2O	GA	0.3	TEDA	48
	0.4 g TEDA	H_2O	GA	0.4	TEDA	48
Synthesis time	24h	H_2O	GA	0.5	TEDA	24
	72h	H_2O	GA	0.5	TEDA	72

[#] *- For comparison reasons, the name of the reference sample changes throughout the manuscript, in order to highlight the studied parameter; this sample is present in each set of studied parameters. * - cross-linker*

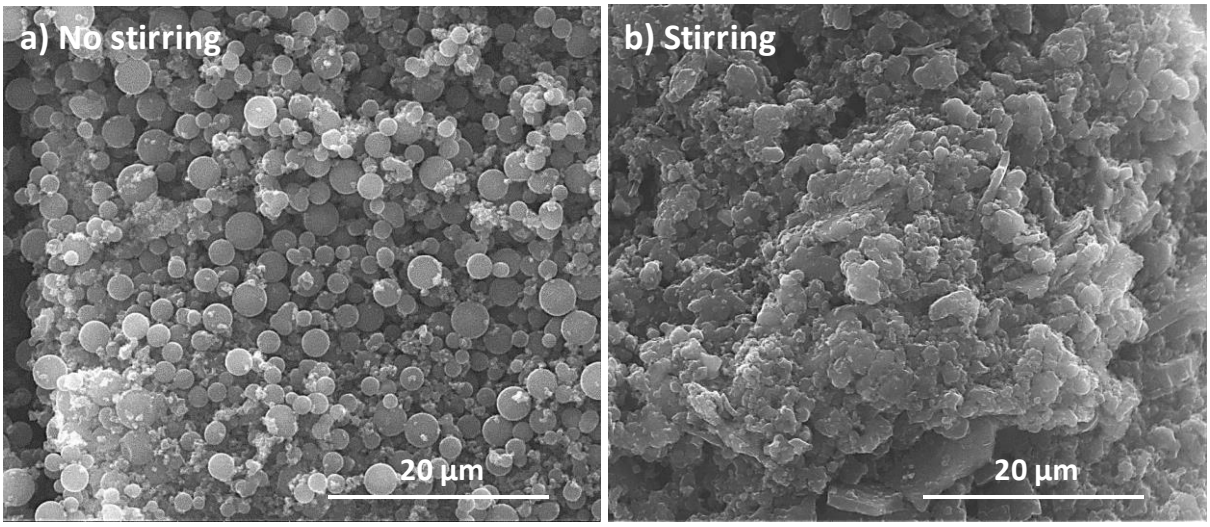

Figure S2: SEM images of carbon spheres obtained using Mimosa-MC precursor: (a) no stirring and (b) under stirring during the reaction.

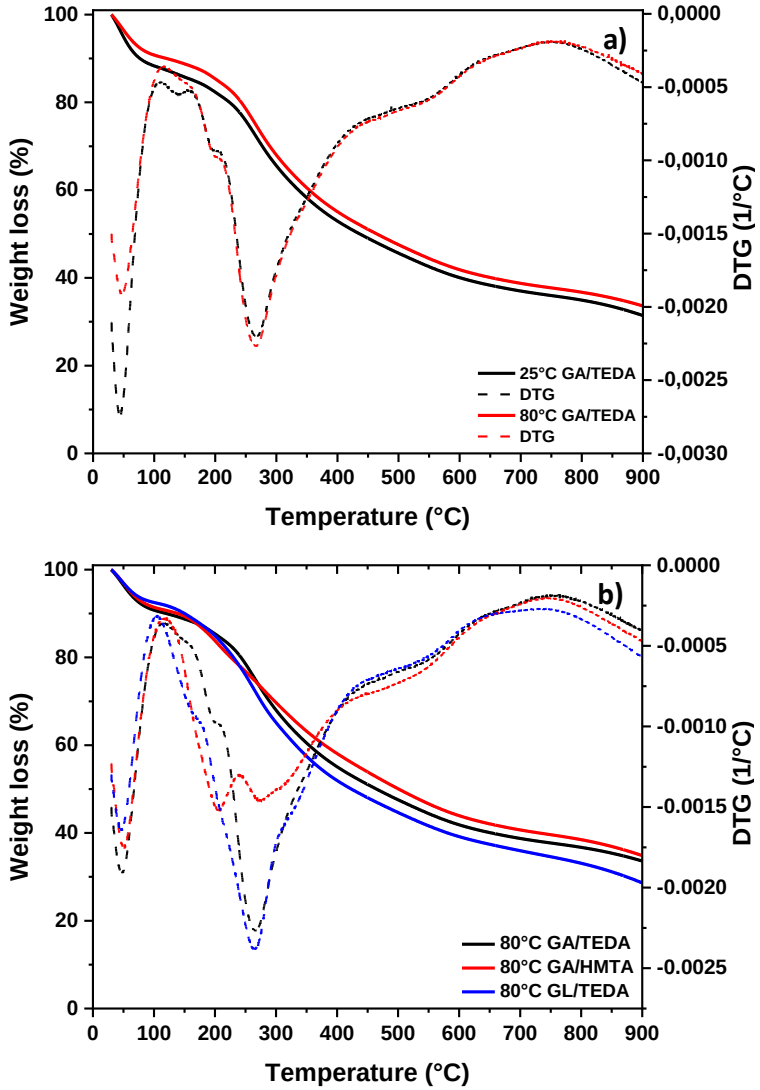

Figure S3: TGA/DTG profiles of the polymers obtained with Mimosa-MC precursor using water solvent and a) GA/TEDA cross-linkers at 25 °C and 80 °C; b) with different type of cross-linker (GA/TEDA, GA/HMTA, GL/TEDA) in the reaction mixture at 80 °C.

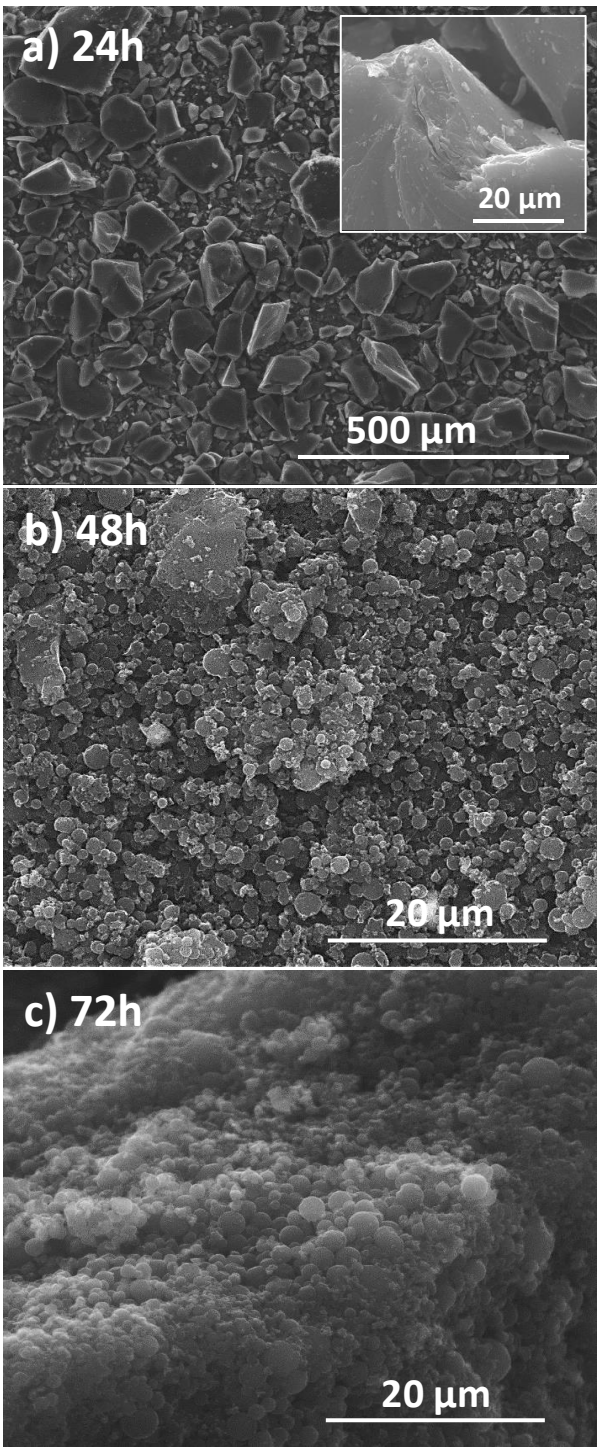

Figure S4: SEM images of carbon spheres obtained using Mimosa-MC precursor by varying the synthesis time: a) 24h (), b) 48h and c) 72h.

The elemental composition of polyphenol spheres and hard carbon materials was carried out with an Vario EL Cube CHNS Elemental Analyzer. The analyses were carried out under helium flow by burning the samples at 1100 °C. The released gases are further reduced (~850 °C), to CO_2, SO_2, H_2O and NO_x and then analysed by a thermal conductivity detector (TDC), by measuring the variation in the thermal conductivity of the gases to determine the CHNS composition. The oxygen amount was estimated by difference (100% - % CHNS), however, it should be mentioned that some inorganics are present in the materials (Table S2) and not taken into consideration.

Table S2. Chemical composition determined by elemental analysis on both polymer spheres and hard carbon materials along with the % of fixed carbon determined for the HCs.

Material	**Elemental composition (wt%)**					**Fixed C**
	C	**H**	**N**	**S**	**O***	**%**
Catechu	49.68	5.39	6.25	0.08	38.61	-
Mimosa MC	51.93	5.27	5.79	0.06	36.96	-
Mimosa MG	51.28	5.36	6.02	0.27	37.07	-
HC-C1500	97.20	0.23	0.22	0.26	2.09	68.5
HC-MC1500	99.27	0.12	0.24	0.24	0.13	70.7
HC-MG1500	98.26	0.09	0.37	0.11	1.16	72.8
HC-MG1600	99.47	0.09	0.21	0.13	0.10	73.9

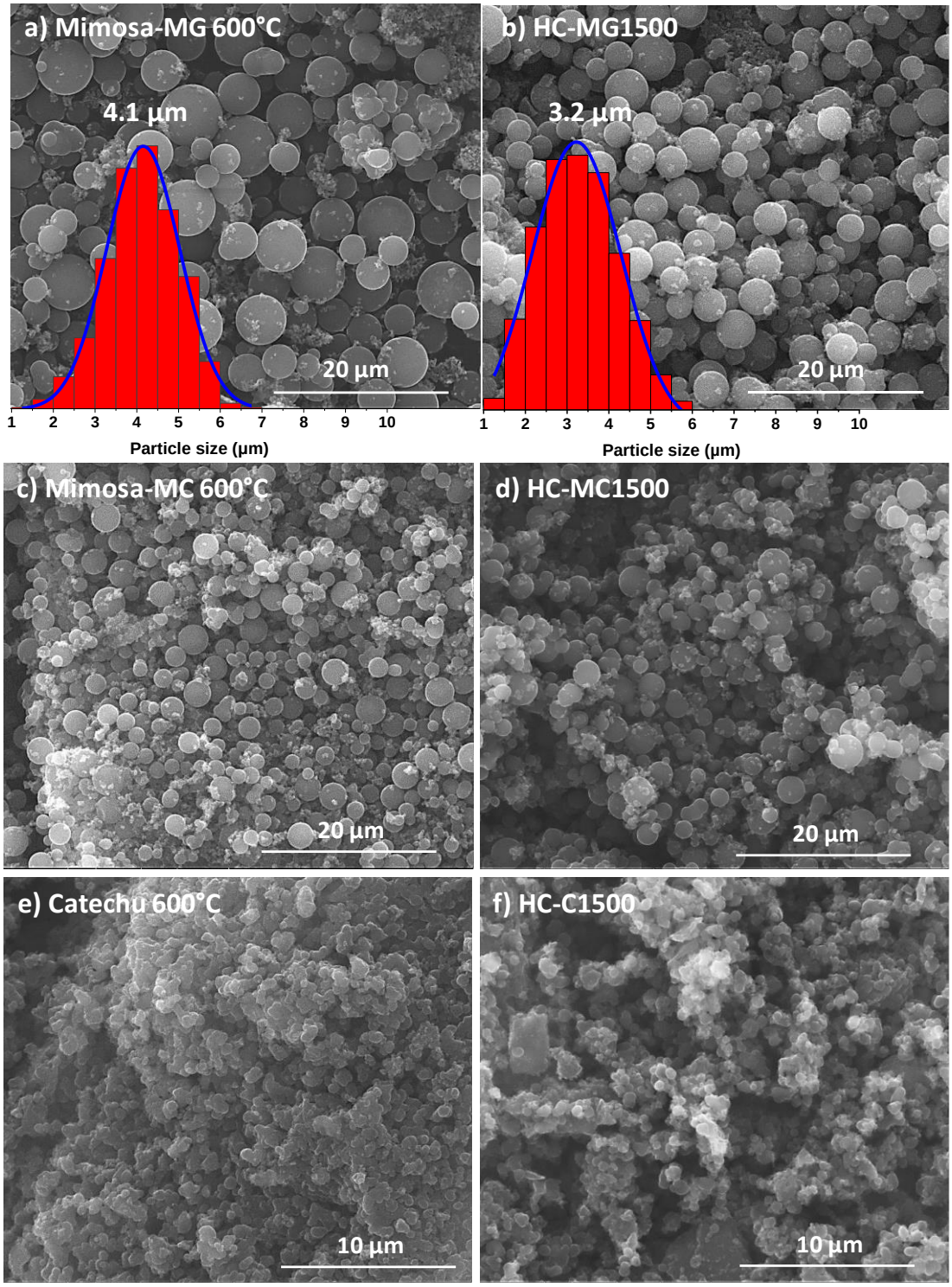

Figure S5: SEM images of carbon spheres obtained using Mimosa-MG precursor at different temperatures: a) 600 °C and b) 1500 °C. Inset: particles size distribution of the two materials. The micrographs of Mimosa-MC at c) 600 °C and d) 1500 °C and Cachou at e) 600 °C and f) 1500 °C.

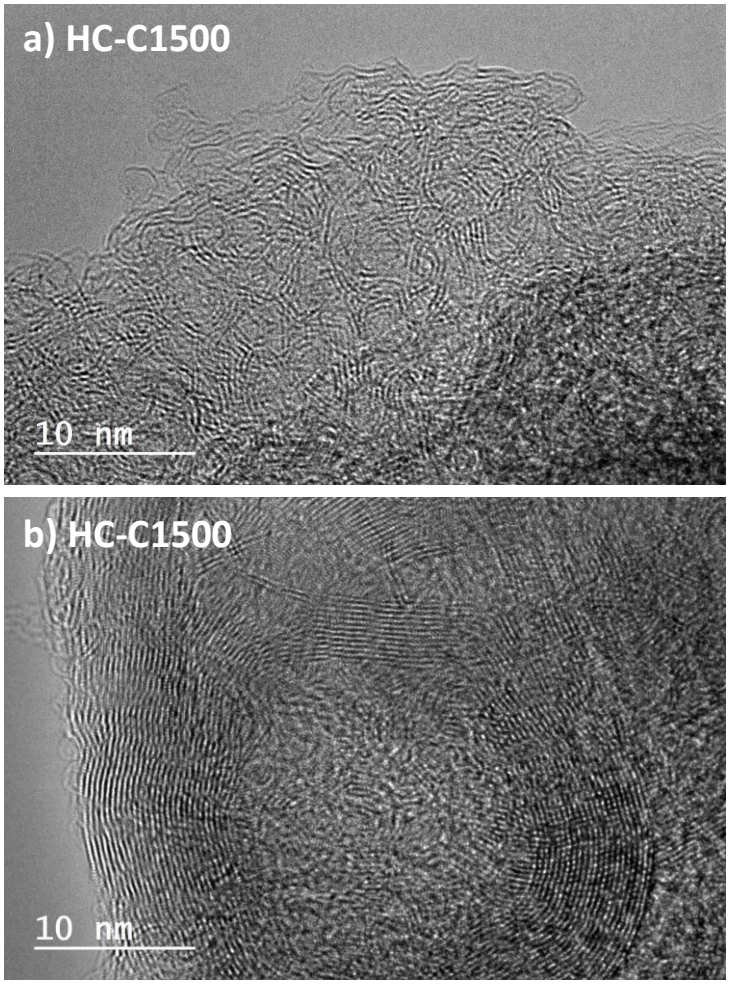

Figure S6: HR-TEM images of HC-C1500 material revealing the heterogeneous structure: a) disordered area and b) highly graphitized area.

Table S3. Pycnometric (He) densities, total pore volumes determined by N_2 adsorption (V_{OP}), ratios of closed porosity (R_{CP}) and open pores (R_{OP}) and solid phase for hard carbon materials.

HC	d_{He} (g cm^{-3})	V_{OP} N_2 (cm^3 g^{-1})	R_{CP} (%)	R_{OP} (%)	Solid phase (%)
HC-C1500	1.97	0.0141	14.67	2.70	82.61
HC-MC1500	2.10	0.0064	09.35	1.32	89.31
HC-MG1500	2.05	0.0069	11.47	1.39	87.12
HC-MG1600	1.88	0.0070	18.71	1.29	79.98

Table S4. EDX chemical composition of the hard carbon materials

Elements	HC-C1500	HC-MC1500	HC-MG1500	HC-MG1600
C	91.91	92.25	91.87	93.60
O	6.97	7.34	7.53	5.77
Na	-	-	-	-
K	0.26	0.31	0.26	0.23
Ca	0.50	0.10	0.19	0.25
P	0.20	-	0.1	0.15
Al	-	-	0.05	-
Si	0.16	-	-	-
Total	**100 (Weight %)**			

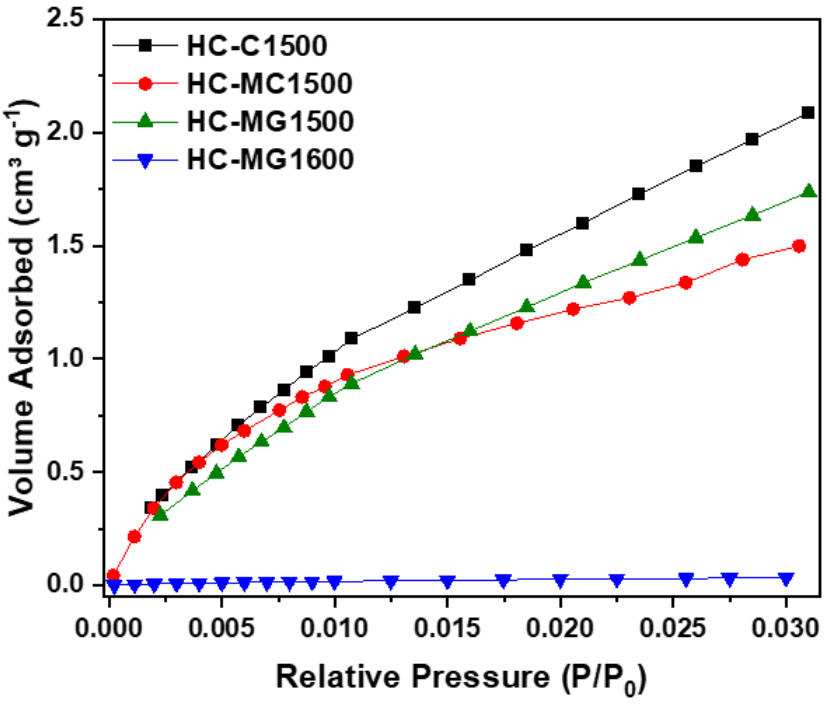

Figure S7: CO_2 adsorption isotherms at 273K of the HC materials.

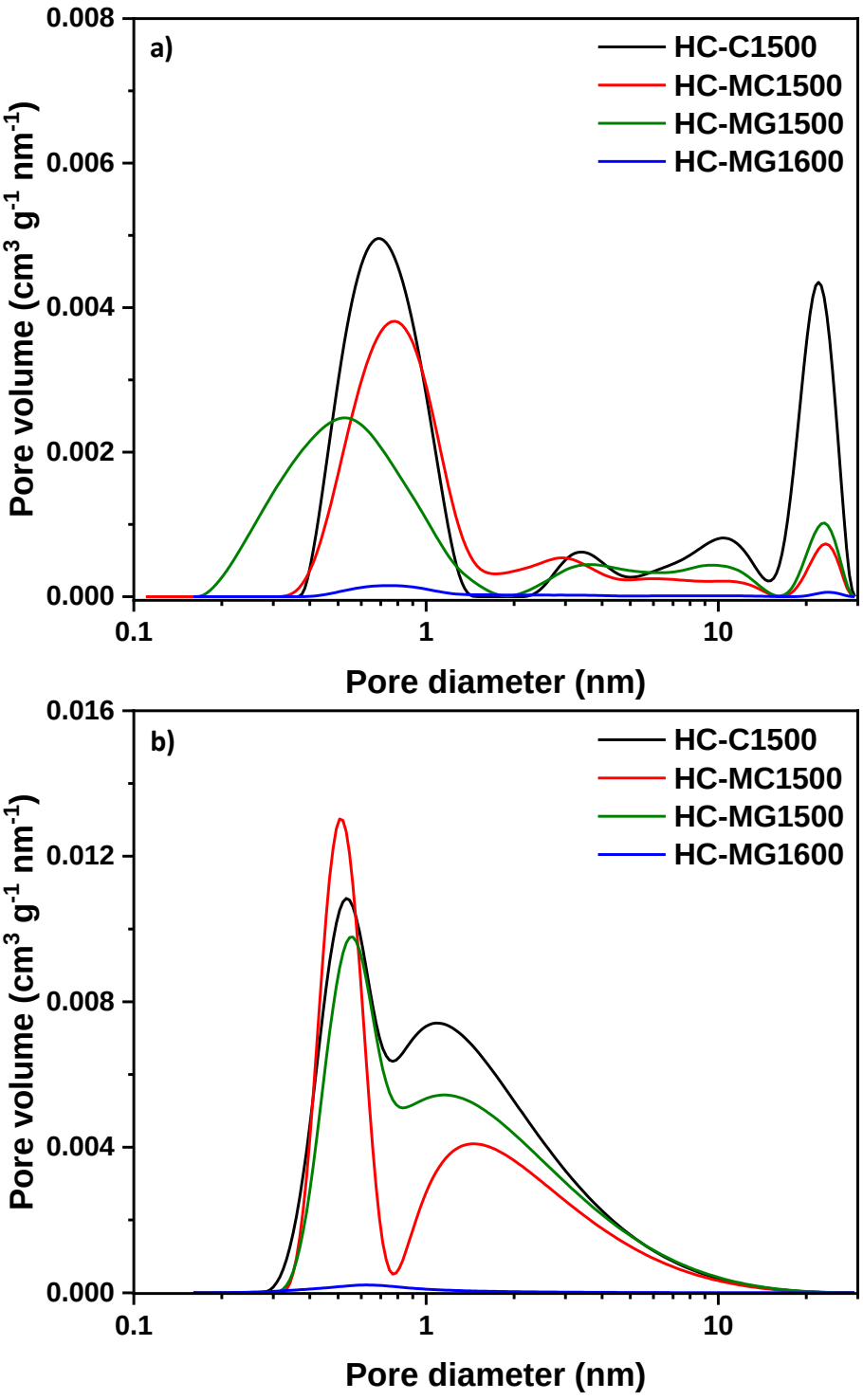

Figure S8: N_2 and CO_2 pore size distributions (log scale) determined by 2D-NLDFT theory

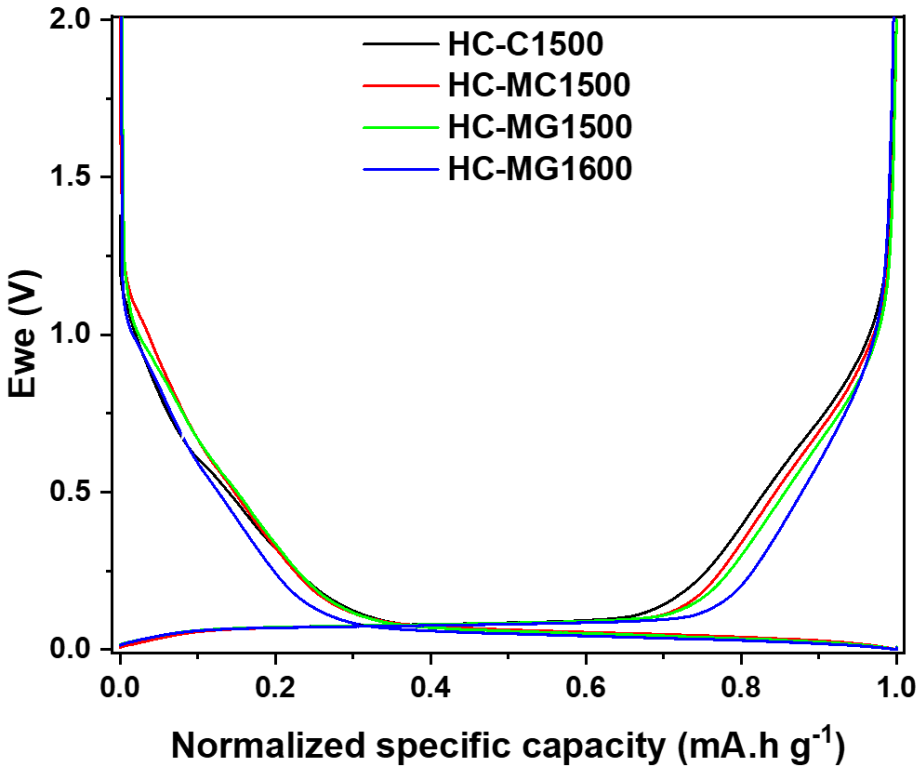

Figure S9: Normalized discharge–charge profiles of the HCS materials during the first charge/discharge cycle

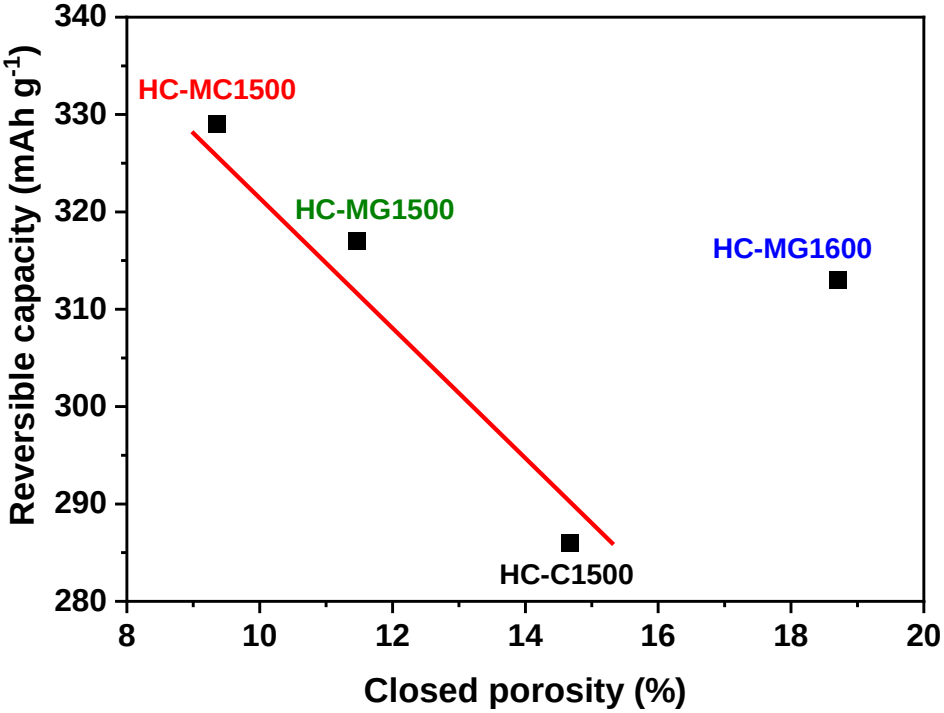

Figure S10: Correlation between reversible capacity of the HC materials and the closed porosity.

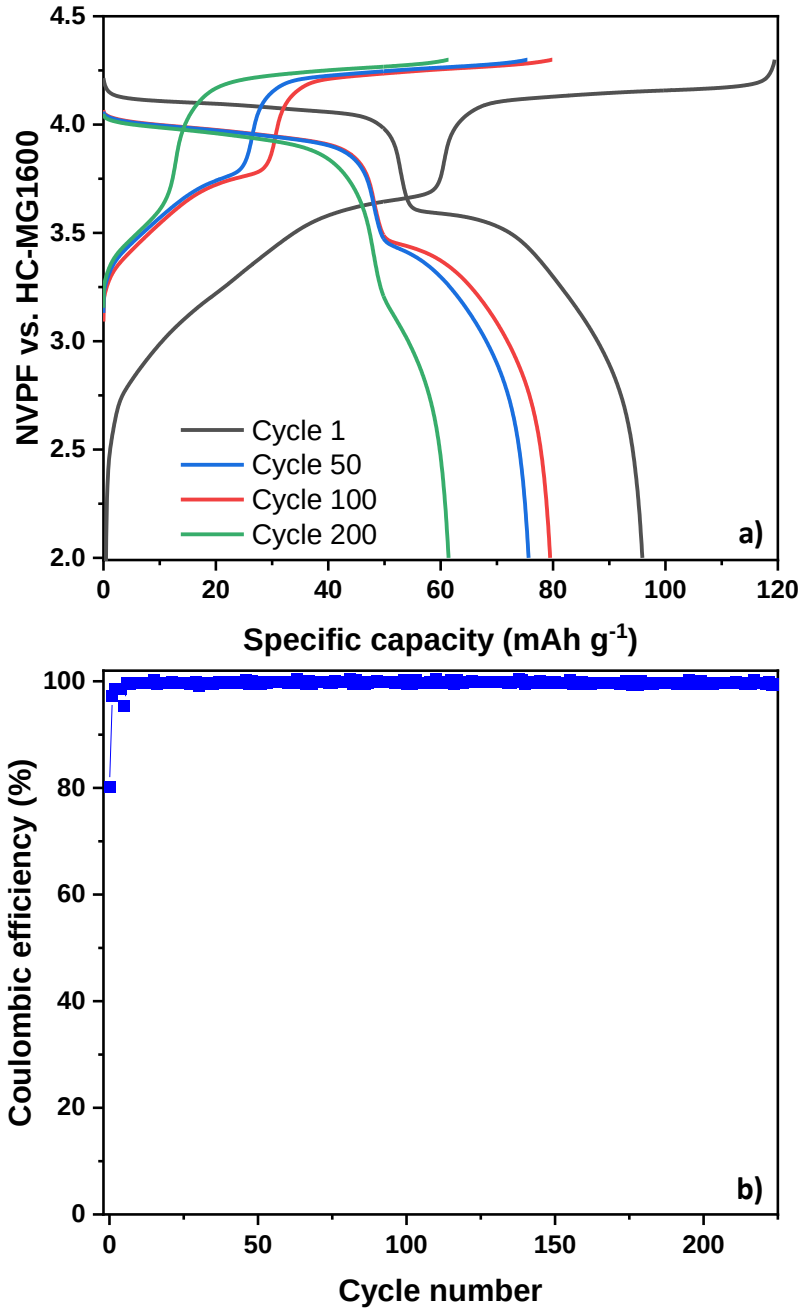

Figure S11: a) Full-cell retention of NVPF (vs. HC-MG1600) specific capacity at 1C after the 1st, 50th, 100th and 200th cycle. b) Coulombic efficiency evolution of the full-cell over cycling.

Precursor	Remarks on the precursors/synthesis	Mass loading (mg cm^{-2})	Electrode formulation AM:B:CC [c]	Electrolyte	Current density (mA g^{-1})	ICE (%)	Rev. capacity (mAh g^{-1})	Ref.
Lotus stem	Used as food	1.0	90:10:00	1M $NaClO_4$ in EC:DEC	40	70	350	[1]
Wine corks waste	HCl treatment; Limited access	2.5 - 3.5	90: 5: 5	1M $NaPF_6$ in EC:DMC	30	81	358	[2]
Garlic	Expensive; Food	~ 1.0	75:10:15	1M $NaClO_4$ in EC:DEC	50	50.7	260	[3]
Camphor wood residues	Pre-treatment at 300 °C; HCl washing after TT	~ 1.0	80:10:10	1M $NaClO_4$ in EC:DMC	20	83	324	[4]
Lotus leaves	HTC [b] 1M HCl	2.3	80:10:10	1M $NaClO_4$ in PC:DEC	50	67	270	[5]
Sugarcane	$NaOH/NaClO_2$ washing	-	80:10:10	1M $NaClO_4$ in EC:PC	100	78.2	229	[6]
Sucrose	H_2SO_4 dissolution	~ 1.0	80:10:10	1M $NaPF_6$ in EC:PC	20	71.4	275	[7]
Milled-wood lignin	Cheap; simple annealing	1.1 - 1.3	80:10:10	1M $NaPF_6$ in EC:DEC	20	80	293	[8]
Microcrystalline cellulose	Cheap; simple annealing	1.1 - 1.3	80:10:10	1M $NaPF_6$ in EC:DEC	20	87.3	343	[8]
Phloroglucinol	Expensive	5.0 - 10.0	94: 3: 3	1M $NaPF_6$ in EC:DMC	7.4	92	300	[9]
Phenolic resin	Pre-treatment at 300 °C; Expensive/toxic [a]	3.0 - 4.0	90: 5: 5	1M $NaPF_6$ in EC:DEC	20	80.7	310	[10]
Tannin extract	Toxic Formaldehyde	3	92:2.6+2.5 [d]:2.9	1M $NaPF_6$ in EC:DMC	37.2	87	306	[11]
HC-MC (tannin)	Cheap; simple annealing	3.0 - 5.0	90: 5: 5	1M $NaPF_6$ in EC:DMC	37.2	85.4	295	[12]
HC-MG (tannin)	Cheap; simple annealing	3.0 - 5.0	90: 5: 5	1M $NaPF_6$ in EC:DMC	37.2	85.5	300	[12]
HC-MC1500 (tannin)	Sol-gel step	5.0 - 10.0	94: 3: 3	1M $NaPF_6$ in EC:DMC	37.2	85	329	*here*
HC-MG1600 (tannin)	Sol-gel step	5.0 - 10.0	94: 3: 3	1M $NaPF_6$ in EC:DMC	37.2	88	313	*here*

Table S5. Comparison between recently reported hard carbons in the literature and the best materials reported in this work. Different practical aspects were considered including the precursor origin and synthesis conditions, mass loading and electrode formulation, electrolyte, current density, and the electrochemical performance delivered, i.e., iCE and reversible capacity.

[a] not mentioned in the article the exact origin/synthesis procedure of the phenolic resin

[b] HTC – hydrothermal carbonization

[c] AM = active material; B = binder; CC = conductive carbon.

[d] 2.5% of Triton X-100 (surfactant)

References

1 N. Zhang, Q. Liu, W. Chen, M. Wan, X. Li, L. Wang, L. Xue and W. Zhang, *Journal of Power Sources*, 2018, **378**, 331–337.

2 Y. Li, Y. Lu, Q. Meng, A. C. S. Jensen, Q. Zhang, Q. Zhang, Y. Tong, Y. Qi, L. Gu, M.-M. Titirici and Y.-S. Hu, *Advanced Energy Materials*, 2019, **9**, 1902852.

3 H. Liu, X. Liu, H. Wang, Y. Zheng, H. Zhang, J. Shi, W. Liu, M. Huang, J. Kan, X. Zhao and D. Li, *ACS Sustainable Chem. Eng.*, 2019, acssuschemeng.9b01370.

4 S. Guo, Y. Chen, L. Tong, Y. Cao, H. Jiao, Z. long and X. Qiu, *Electrochimica Acta*, 2022, **410**, 140017.

5 C.-C. Wang and W.-L. Su, *ACS Appl. Energy Mater.*, 2022, **5**, 1052–1064.

6 M. Kim, J. F. S. Fernando, Z. Li, A. Alowasheeir, A. Ashok, R. Xin, D. Martin, A. Kumar Nanjundan, D. V. Golberg, Y. Yamauchi, N. Amiralian and J. Li, *Chemical Engineering Journal*, 2022, **445**, 136344.

7 Y. Huang, Y. Wang, P. Bai and Y. Xu, *ACS Appl. Mater. Interfaces*, 2021, **13**, 38441–38449.

8 X.-S. Wu, X.-L. Dong, B.-Y. Wang, J.-L. Xia and W.-C. Li, *Renewable Energy*, 2022, **189**, 630–638.

9 A. Beda, F. Rabuel, M. Morcrette, S. Knopf, P.-L. Taberna, P. Simon and C. M. Ghimbeu, *J. Mater. Chem. A*, 2021, **9**, 1743–1758.

10 Z. Wei, H.-X. Zhao, Y.-B. Niu, S.-Y. Zhang, Y.-B. Wu, H.-J. Yan, S. Xin, Y.-X. Yin and Y.-G. Guo, *Mater. Chem. Front.*, 2021, **5**, 3911–3917.

11 H. Tonnoir, D. Huo, R. L. S. Canevesi, V. Fierro, A. Celzard and R. Janot, *Materials Today Chemistry*, 2022, **23**, 100614.

12 A. Beda, A. M. Escamilla-Pérez, L. Simonin and C. Matei Ghimbeu, *ACS Appl. Energy Mater.*, 2022, **5**, 4774–4787.